

# Dynamics around a hydrogen bond – The dynamics of UV excited acetic acid dimers

Contact [r.s.minns@soton.ac.uk](mailto:r.s.minns@soton.ac.uk)

**E. Plackett, R. S. Minns**

*School of Chemistry, University of Southampton  
Highfield Campus, Southampton, SO17 1BJ, United Kingdom*

**H. McGhee, R. Ingle,**

*Department of Chemistry, University College London  
20 Gordon Street, London WC1H 0AJ, United Kingdom*

**G. M. Greetham, G. Karras, I. V. Sazanovich**

*Central Laser Facility, Research Complex at Harwell,  
Didcot, Oxon, OX110QX, United Kingdom*

**C. Robertson, A. De Matos Loja, M. Patterson**

*Institute of Chemical Sciences, School of Engineering and  
Physical Sciences, Heriot-Watt University, Edinburgh, Scotland,  
United Kingdom*

## Introduction

The absorption of a high energy UV photon (4-6 eV) by a molecule changes the electronic (bonding) forces that control molecular structure. This often leads to photochemical reactions involving the breaking and making of chemical bonds. Subtle changes to weak non-covalent interactions of the molecule cause significant changes in the dynamics. For example, the addition of a single hydrogen bond (HB) can completely switch off the dominant photochemical processes in an isolated molecule, reducing it to an insignificant contribution in a molecule bound to another by a HB.[1] The HB therefore opens an alternative reaction pathway often initially localised on the HB itself. As the strength of a HB is on the order of 5 % of a typical covalent bond, and only a few percent of the UV photon energy, it is perhaps surprising that it would have any significant effect on photochemical mechanisms and outcomes. Repeated measurements have unquestionably shown this HB effect but have provided little explanation of the relative efficacy of a specific HB structure so far.[1,2,3]

Recent reanalysis of HBs in terms of the underlying electrostatics provides a new approach to these photochemical questions. Measurements of the vibrational Stark effect in the electronic ground state have shown that a single HB can generate electric field strengths of 30-100 MV cm<sup>-1</sup>, while electric fields of several hundred MV cm<sup>-1</sup> are measured where multiple, highly directional HBs work in tandem.[4,5,6] The effect of these electrostatic forces on ground state (thermal) processes has been at the centre of large scale research in understanding enzyme and protein function, with the first extension of this idea to the control of photoisomerisation processes in fluorescent proteins recently published [7]. The photoisomerisation study used systematic changes to the steric and electrostatic environment to explore the relative effects of these on the photodynamics. To the best of our knowledge there have been no such studies of molecular scale systems where the effect of the stark fields on the underpinning mechanism/reaction pathway have been explored explicitly.

As a first experiment to explore this effect we have measured the dynamics of UV excited acetic acid dimers and trifluoroacetic acid dimers to explore how the changing field strength affects the dynamics in the two species. Here we focus on our preliminary analysis of the time-resolved infrared (TRIR) measurements of the acetic acid dimer and leave analysis of the transient electronic measurements and the measurements on trifluoroacetic acid for a future publication.

## Experimental Description

Femtosecond TRIR absorption experiments were performed using the ULTRA system at the Central Laser Facility (CLF). The setup has been fully described elsewhere [8] such that we only provide brief details here. The acetic acid dimers were pumped with 100 nJ of 200 nm radiation generated through

sequential second harmonic and sum frequency generation processes of the 800 nm output of a Ti:Sapphire laser system. The broad band mid-IR probe pulses were produced using a commercial fs-OPA (LightConversion) resulting in a bandwidth of ~400 cm<sup>-1</sup> at the 1700 cm<sup>-1</sup> and 1300 cm<sup>-1</sup> regions measured. The resultant pump-probe pulses gave an instrument response function of <500 fs full width at half maximum. An optical chopper was positioned in the pump beam path, blocking alternate pump pulses, allowing for shot-to-shot comparison of the pump plus probe signal to the probe only signal. Measurements were taken at pump-probe delays between -5 and 3000 ps.

The pump and probe pulses are crossed at a small angle through the sample cell with the polarisation of the pump relative to the probe set to the magic angle. The beam diameters of the pump and probe through the sample were 150 and 100 μm respectively. The sample solution was pumped through a Harrick cell equipped with CaF<sub>2</sub> windows and 50 μm PTFE spacers. The Harrick cell was rastered in the x and y axes, perpendicular to the beam propagation direction, to minimize any thermal effects incurred from pump and probe beams travelling through the CaF<sub>2</sub> windows.

After passing through the sample the probe spectrum is simultaneously monitored using two 128-element Mercury cadmium telluride detectors (IR associates). The two detectors measure slightly shifted regions of the full spectrum with the spectral ranges slightly overlapping at a particular region of interest, providing two sets of data to compare against each other. The spectrum is calibrated through comparison to a reference spectrum of polystyrene.

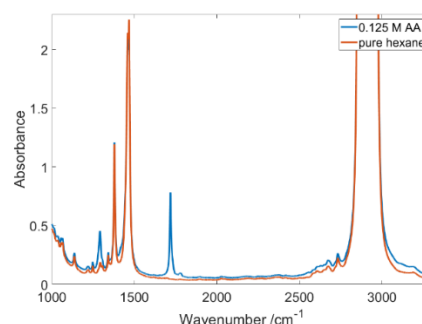


**Figure 1.** FTIR of 0.125 M acetic acid in hexane and of pure hexane. The key regions of the spectrum

## Results

The Fourier Transform IR spectrum of acetic acid in hexane is plotted in figure 1 along with the FTIR of pure hexane. The spectrum contains two regions that have strong IR absorption bands that are relatively clear of hexane contributions. The peaks at 1720 cm<sup>-1</sup> and 1290 cm<sup>-1</sup> relate to the carbonyl stretch and in-

plane ring wag vibrations respectively. TRIR absorption measurements were performed over these two regions. We also attempted measurements at the OH stretch around  $3000\text{ cm}^{-1}$  however, we could not recover a reliable time dependent signal in this region. The TRIR absorption spectra at pump-probe delays up to 10 ps around  $1700\text{ cm}^{-1}$  and  $1300\text{ cm}^{-1}$  are plotted in figure 2 and figure 3 respectively.

Around time zero, the  $1700\text{ cm}^{-1}$  spectrum shows an apparent splitting of the ground state peak with enhanced absorption on either side of the ground state maximum at  $1719\text{ cm}^{-1}$ , figure 2. In order to analyse the changes in intensity across the various regions of the spectrum we integrate the OD changes at three regions that cover the central energy of the ground state transition and the enhancements observed to the red and the blue of this. The integrated intensity across the three regions are plotted in figure 4. Each region shows the same temporal profile with an increase in the measured  $\Delta\text{OD}$  that oscillates with a characteristic frequency for the first few picoseconds. The enhancement is also observed at the ground state energy but with a much lower OD enhancement. The oscillations have a period of approximately 4 ps and damp out over the course of the first 5 ps. The remaining signal decays back to zero with an exponential time constant of  $\sim 60\text{ ps}$ .

The data around  $1300\text{ cm}^{-1}$  shows a similar initial splitting of the ground state peak with new features appearing to the red and the blue of the central frequency of the ground state vibration, figure 3. The intensity profiles are plotted in figure 5 and highlight that the new features ( $1268\text{-}1281\text{ cm}^{-1}$ ) decay rapidly with the reformation of a more intense peak at the same energy as the ground state vibration ( $1286\text{-}1300\text{ cm}^{-1}$ ). The intensity profile of the peak centred at  $1293\text{ cm}^{-1}$  reaches the second maximum at 1.7 ps and subsequently decays with an exponential time constant of approximately 800 ps.

The dynamics of the signals at the two regions show strong similarities in the initial splitting of the peaks with increased intensity to the red and the blue of the central energy but also significant differences in the time profiles of these features that correlate with different parts of the dynamics at play.

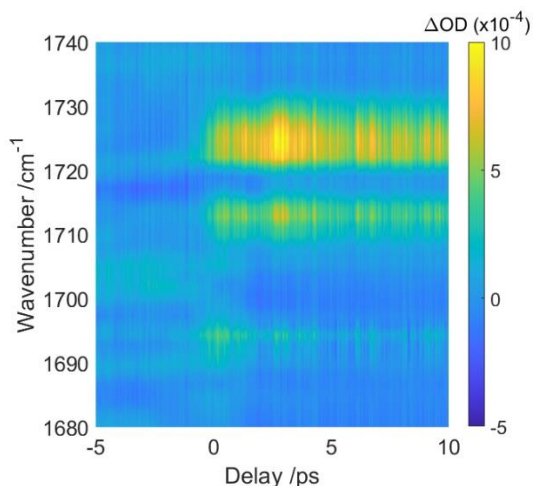


**Figure 2.** TRIR spectrum of acetic acid in hexane around the carbonyl stretch.

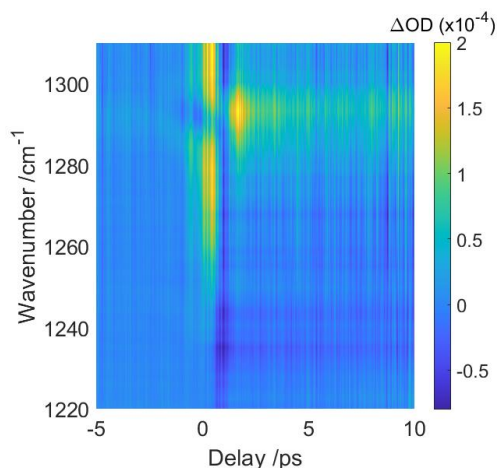


**Figure 3.** TRIR spectrum of acetic acid in hexane around the ring wag vibration.

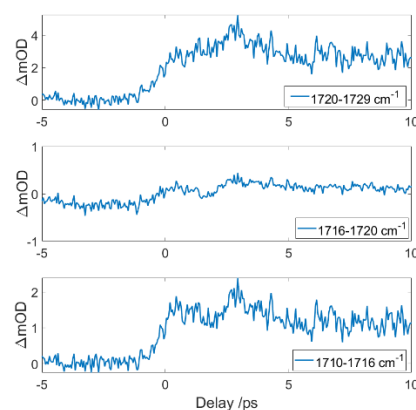


**Figure 4.** Integrated optical density changes over three energy ranges around the carbonyl stretch wavenumber. Integrated regions are given in the legends.

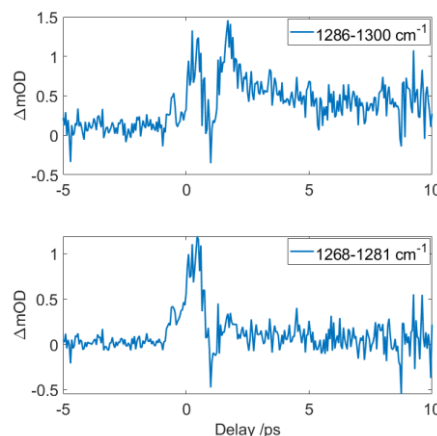


**Figure 5.** Integrated optical density changes over three energy ranges around the ring wag vibrational wavenumber. Integrated regions are given in the legends.

In order to interpret the observed changes, we have performed some preliminary calculation of the excited state potentials and the critical geometries associated with the relaxation dynamics. The potential energy surfaces are calculated at the CAS(8,6) level using 3-21G basis. The scan while preliminary is qualitatively correct with critical geometries of the conical intersections and minima (for the  $S_2/S_1$  and  $S_1$  minima) matching those calculated at the TDDFT with 6-311G(d,p) level.

200 nm excitation leads to population transfer into the optically bright  $S_2$  state. The  $S_2$  and  $S_1$  states are degenerate with the initial dynamics along the  $S_2$  surface leading to a skewing of the hydrogen bonds, while remaining flat, creating a "skewed" rhombus structure at the position of the lowest energy conical intersection between the  $S_2$  and  $S_1$  surfaces. Population transfer onto the  $S_1$  surface provides access to a new energy minimum related to a buckled ring structure where the planarity of the system is lost. At even more buckled structures there is also a  $S_1/S_0$  conical intersection leading to the reformation of the ground state.

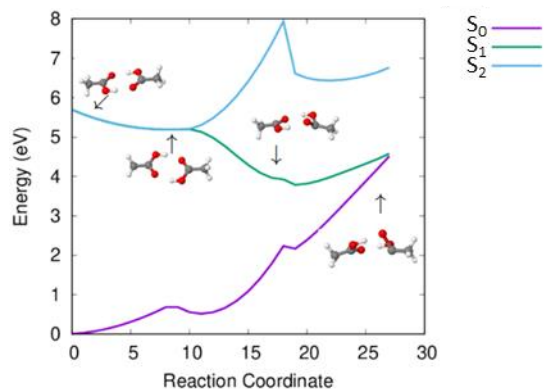


**Figure 6.** Minimum energy path cuts along the potential energy surfaces of the acetic acid dimer showing the key structural changes as the molecules relaxes back to the electronic ground state.

The calculations suggest that the skewed planar geometry is reached within a few  $10^3$  of fs, while it will take significantly longer (at least 500 fs) to reach the buckled geometry related to the  $S_1$  minimum. The calculated IR cross-section around  $1290\text{ cm}^{-1}$  show significant enhancements at higher energies at the skewed geometry. We therefore suggest the initial splitting of the of the  $1290\text{ cm}^{-1}$  peak and rapid decay of the blue and red shifted components is associated with population of the skewed geometry with the decay in this signal related to the buckling of the dimer over the course of the first ps. The long-lived signals then relate to relaxation of the buckled geometry and eventual reformation of the ground state on a much longer timescale.

Ongoing calculations are focusing on the dynamics responsible for the longer timescale oscillations observed in the  $1700\text{ cm}^{-1}$  region and the eventual reformation of the ground electronic state.

## Conclusions

We have measured the relaxation dynamics of acetic acid dimers following deep UV excitation. The results have been combined with ab-initio calculations of the excited state potentials leading to the following preliminary assignment of the dynamics. Following excitation, the initial dynamics in the  $S_2$  excited state lead to ring deformation and a skewed planar structure of the hydrogen bonded ring. The dimer then passes through a conical intersection onto the  $S_1$  electronic state where it is seen to break the planar structure and buckle.

## Acknowledgements

We gratefully acknowledge financial support from the Royal Society through award RGF\EA\180111.

## References

1. D. A. Horke, *et al.*, Phys. Rev. Lett. **117** 163002 (2016).
2. K. Röttger, *et al.*, Angew. Chem. Int. Ed. **15** 14719 (2015).
3. B. Marchetti, *et al.*, Phys. Chem. Chem. Phys., **18**, 20007 (2016).

4. S. D. Fried and S. G. Boxer, Annual Reviews of Biochemistry **86**, 387 (2017).
5. S. D. Fried and S. G. Boxer, Acc. Chem. Res. **48**, 998 (2015).
6. S. D. Fried, S. Bagchi, and S. G. Boxer, Science **346** 1510 (2014).
7. Romei, *et al.* Science **367**, 76 (2020).
8. Greetham *et al.* Applied Spectroscopy. **64**, 1311, (2010)